AGU ADVANCING EARTH AND SPACE SCIENCE

Geophysical Research Letters

RESEARCH LETTER
10.1029/2023GL103523

550-Year Climate Periodicity in the Yunnan-Guizhou Plateau During the Late Mid-Holocene: Insights and Implications

Youwei Li[1,2], Dominik Fleitmann[3], Xiangli Wang[4], Carlos Pérez-Mejías[1], Lijuan Sha[1], Xiyu Dong[1], Deyuan Wang[2], Rui Zhang[1], Xiaoli Qu[5], and Hai Cheng[1,6]

[1]Institute of Global Environmental Change, Xi'an Jiaotong University, Xi'an, China, [2]Institute of Mountain Resources, Guizhou Academy of Sciences, Guiyang, China, [3]Department of Environmental Sciences, University of Basel, Basel, Switzerland, [4]College of History and Culture, Hebei Normal University, Shijiazhuang, China, [5]State Key Laboratory for Manufacturing Systems Engineering, Xi'an Jiaotong University, Xi'an, China, [6]State Key Laboratory of Loess and Quaternary Geology, Institute of Earth Environment, Chinese Academy of Sciences, Xi'an, China

Key Points:

- A significant multi-centennial temperature and vegetation oscillation of ~550-yr cycles occurred between ~5,870 and ~3,670 years ago in the Yunnan-Guizhou Plateau (YGP)
- The climate cycles were likely linked to the Atlantic meridional overturning circulation variation through coupled oceanic-atmospheric processes
- The first cold phase of the ~550-yr cycles in our records coincided with a change of population and major cultural transform in the YGP at ~5,500–5,000 years ago, implying a critical role of climate change and resource shortage in the prehistorical cultural evolution in the region

Supporting Information:

Supporting Information may be found in the online version of this article.

Correspondence to:

H. Cheng,
cheng021@xjtu.edu.cn

Citation:

Li, Y., Fleitmann, D., Wang, X., Pérez-Mejías, C., Sha, L., Dong, X., et al. (2023). 550-year climate periodicity in the Yunnan-Guizhou Plateau during the late mid-Holocene: Insights and implications. *Geophysical Research Letters*, *50*, e2023GL103523. https://doi.org/10.1029/2023GL103523

Received 2 MAR 2023
Accepted 22 MAY 2023

Author Contributions:

Conceptualization: Youwei Li, Xiangli Wang, Hai Cheng
Data curation: Youwei Li, Xiaoli Qu
Formal analysis: Youwei Li, Dominik Fleitmann, Xiaoli Qu
Funding acquisition: Youwei Li, Hai Cheng

Abstract Significant multi-centennial climate oscillations have been documented in a number of well-dated climate records across the Holocene epoch and left various imprints in human cultural history. In this study, we developed speleothem $\delta^{13}C$, $\delta^{18}O$, trace elements, and lamina thickness records from the Yunnan-Guizhou Plateau (YGP). Our high-resolution and precisely dated records show a significant ~550-yr cycle as the dominant pattern of regional temperature and vegetation variations between ~5,870 and ~3,670 years ago. The phase analyses of the 550-yr cycles among our speleothem records, other Northern Hemisphere climate records, solar activity index, and Atlantic meridional overturning circulation (AMOC) variations suggest that this climate cycle has a large spatial extent, and may be causally linked to the AMOC changes through coupled oceanic-atmospheric processes. Additionally, the first cold phase of the ~550-yr cycle in our records coincides with the major cultural development on the YGP at ~5,500–5,000 years ago, suggesting a critical relationship between climate and prehistorical cultural changes in the region.

Plain Language Summary This study presents precisely dated speleothem isotope and lamina thickness records, which shows a ~550-yr periodicity of vegetation and temperature changes between ~5,870 and ~3,670 years ago in the Yunnan-Guizhou Plateau (YGP), southwestern China. The phase analyses between our records and other Northern Hemisphere climate records suggest that these climate cycles have a large spatial scale in Northern Hemisphere and may be linked to the Atlantic meridional overturning circulation changes through coupled oceanic-atmospheric processes. Besides, the records show that a cold phase during ~5,500–5,000 years ago coincided with the period of development of YGP Neolithic production tools, suggesting a critical role of climate change in the prehistorical cultural evolution in the region.

1. Introduction

Multi-centennial-scale climate events (or oscillations) appear to be one of the characteristics of the Holocene climate superimposed on the long-term Holocene evolution history (e.g., Dansgaard et al., 1993; Fleitmann et al., 2003; Kathayat et al., 2017; Y. Wang et al., 2005). Understanding the processes and mechanisms behind these multi-centennial climate events is important for attesting to and improving climate models, and for assessing future climate change as well (e.g., Bakker et al., 2017; McDermott et al., 2001). In the Northern Hemisphere (NH), proxy records from speleothems (e.g., Cheng et al., 2015, 2022; Y. Wang et al., 2005; Zhu et al., 2017), lake sediments (e.g., H. Li et al., 2021; Stebich et al., 2015; Xu et al., 2014, 2019), ice cores (e.g., Stuiver et al., 1995), peatlands (e.g., N. Li et al., 2020) and ocean sediments (e.g., Chapman & Shackleton, 2000; Roth & Reijmer, 2005) have documented ~500–550-yr climate cycles in the Holocene. These cycles may have played an important role in some aspects of Chinese cultural history. As an example, modern climate observations and paleoclimate evidence have shown that the flourishing time of the Tubo Dynasty in the southern Tibetan Plateau, as well as the cultural phases in North China, were closely related to the ~500–550-yr cycles during Holocene (e.g., H. Li et al., 2021; Xu et al., 2019). Therefore, understanding the ~500–550-yr cycle and its forcing factor is an important issue at the research forefront of climate change. Previous palaeoclimatic studies in the Asian summer monsoon region (e.g., Stebich et al., 2015; Xu et al., 2014, 2019, 2020; Zhu et al., 2017) have already revealed a number of quasi 500–550-yr precipitation and/or temperature cycles. However, significant inconsistencies concerning the origin and timing of the 500–550-yr climate periodicity between various regions remain

Investigation: Youwei Li, Xiangli Wang, Deyuan Wang
Methodology: Youwei Li, Dominik Fleitmann, Xiaoli Qu
Project Administration: Youwei Li
Resources: Youwei Li
Supervision: Dominik Fleitmann, Hai Cheng
Validation: Youwei Li
Visualization: Youwei Li
Writing – original draft: Youwei Li, Hai Cheng
Writing – review & editing: Youwei Li, Dominik Fleitmann, Xiangli Wang, Carlos Pérez-Mejías, Lijuan Sha, Xiyu Dong, Rui Zhang, Hai Cheng

unresolved. As such, the reconstruction of high-resolution and precisely dated records that can well characterize the ~500–550-yr cycle is critical to better understand these multi-centennial climate oscillations and their causal relationship to external and internal forcings.

The Yunnan-Guizhou Plateau (YGP) in China is well known for its extraordinary biodiversity, warm and humid climate, and abundance of stone materials and caves, which made it a "paradise for hunter-fisher-gatherers" (Chen, 2020). The Neolithic culture in the region however, appears to be lagging and sporadic compared with other regions in China, which is possibly due to the mountainous and riverine barriers, as well as the superior prehistorical living environments (e.g., Chen, 2019, 2020; K. Li et al., 2014; W. Wang, 2021). Intriguingly, corresponding with the cultural development in the plain areas in China (W. Wu et al., 2017; Xu et al., 2019), multiple lines of evidence (e.g., Chen, 2019, 2020; W. Wang, 2021; Xue et al., 2022) show that the evolution of the tools of production during the Neolithic Age in the YGP widely occurred between ~5,500 and 5,000 years before present (yrs BP, where the "present" is 1950 CE). It has also been suggested that the YGP's prehistorical culture during the mid-Holocene may have been particularly sensitive to climate change due to its large impact on the efficiency of production and the living environment of hunter-fisher-gatherers (e.g., Chen, 2020; Hoelzmann et al., 2001). However, this hypothesis lacks a test from direct paleoclimate evidence.

In this study, we report high-resolution carbon ($\delta^{13}C$)-oxygen isotope ($\delta^{18}O$) and lamina thickness records of speleothem from Guizhouxinv Cave (GZXN) in the YGP, southwestern China, spanning from ~5,870 to ~3,670 yr BP. These records are precisely dated by a combination of U-Th dates and annual lamina accounting results, which allow us to precisely characterize the regional temperature and vegetation variations on a multi-centennial timescale in the context of climate records from the other regions in NH. Our results provide new insights into the ~550-yr climate cyclicity in NH, as well as the possible teleconnection and underlying mechanism. Additionally, in comparison with archeological data, we suggest that the multi-centennial climate oscillations in the YGP region may have played a role in the development of Neolithic production tools during the mid-Holocene period.

2. Cave and Modern Climatology

GZXN (27°4′N, 105°5′E, ~1,000 m above sea level) is located in northwestern Guizhou province, southwestern China (Figure 1). The cave, ~250 m in length, was discovered in 2017 at a depth of ~1,000 m in a newly developed cable tunnel. Due to the well-closed environment, the cave's microclimate is relatively stable, with a temperature of ~16°C and a relative humidity of ~99% (measured by a hand-held hygrometer three times during winter, summer, and spring in 2020 and 2021). The cave site is in eastern Wumeng Mountain. Vegetation types in the area are primarily subtropical evergreen broad-leaved and plateau mountain coniferous forests, dominated by C3-type plants, such as *Pinus, Taxodiaceae*, as well as some shrubs (based on a field survey). Except for some crops planted by the local farmers, no C4-type plants are found in the cave area.

In modern climatology, GZXN Cave is located in the core of the Asian summer monsoon (ASM) region, which is influenced by both the Eastern Asian summer monsoon and the Indian summer monsoon subsystems (e.g., S. Y. Tao & Chen, 1987). The region has a warm and wet climate with an average annual temperature of ~15°C and an average annual precipitation of ~1,050 mm. The majority of the annual precipitation, ~70%, occurs from May to September (MJJAS) during the ASM season (Figure S1a in Supporting Information S1). The precipitation variations in this area is strongly influenced by the El Niño-Southern Oscillation (ENSO), and show diversity in north and northwestern China (see Figure 1 and Text S4 in Supporting Information S1).

In comparison to precipitation, observations show that annual temperature variations in China are more consistent on a large spatial scale (Figure 1b), although there are still regional discrepancies to some extent in the amplitude (e.g., Cao et al., 2013). Previous studies have shown that the increase in the amplitude of mean annual temperature in mainland of China is around 1.12°C over the past 115 years, which is similar to the NH averages (Ding & Dai, 1994; Ren et al., 2017), with one-third of which contributed by the unprecedented level of urbanization (Sun et al., 2016).

3. Materials, Age Model and Results

3.1. Stalagmite Sample

The stalagmite sample (GZXND21-1) was collected in a small cave hall in GZXN in 2021. The sample (~37-cm long), composed of light brown calcite, was cut along the growth axis, and polished (Figure S2 in Supporting

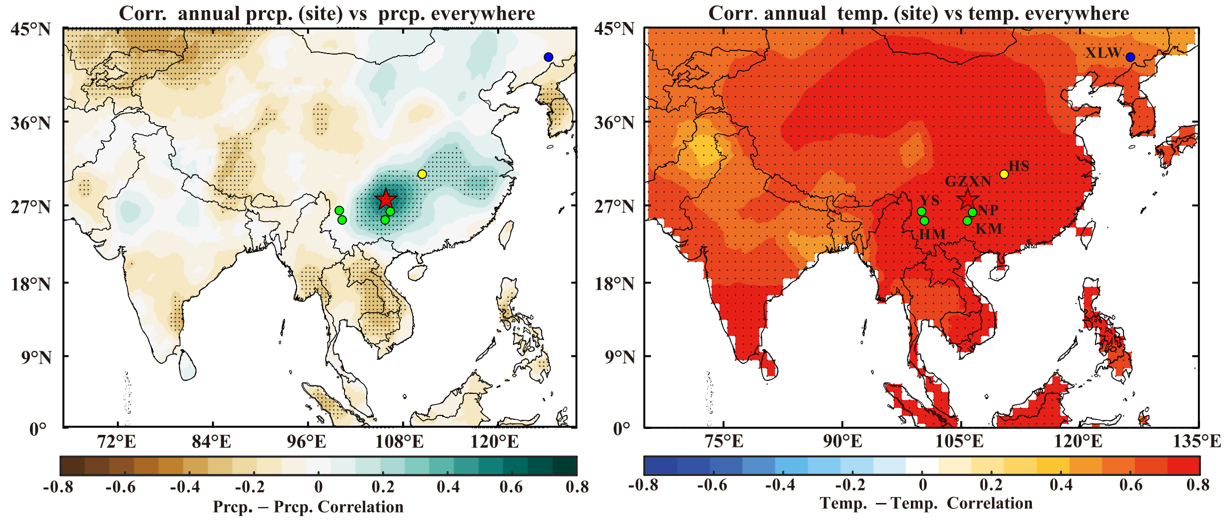

Figure 1. The climate correlation maps between the research site and elsewhere. (a) and (b) The spatial correlations of mean annual precipitation (a) and temperature (b) between the research site and elsewhere (1950–2016). The data are from the Climatic Research Unit (CRU TS v4.05, Harris et al., 2020) with a grid resolution of 0.5 × 0.5° for precipitation and 1 × 1° for temperature. Stipplings indicates a significant correlation ($p < 0.1$ level). The sites of climate records and archaeological sites are labelled: GZXN: Guizhouxinv cave; XLW: Xiaolongwan lake; HS: Heshang cave; NP: Niupo cave site; KM: Kongmingfen site; YS: Yinsuodao site; HM: Haimenkou site.

Information S1). 16 ^{230}Th dating subsamples, 1,342 δ^{13}C and δ^{18}O subsamples, 19 fluorescent images and 1,117 trace element data were analyzed (see Text S1 in Supporting Information S1 for detailed methods). There is no apparent hiatus observed in the fluorescence images of the entire sample.

3.2. Age Model

The stalagmite sample GZXND21-1 has high ^{238}U and low ^{232}Th concentrations (Table S1 in Supporting Information S1). As a result, the errors of the ^{230}Th dates were small (10–28 yr) (Cheng et al., 2013). The age model was reconstructed using the method of least-squares fitting of the annual lamina counting results to the ^{230}Th dates, with uncertainties of ~26 yr (Domínguez-Villar et al., 2012; Dong et al., 2022; Y. W. Li et al., 2022) (Text S2 in Supporting Information S1). The result is consistent with the age model based on the COPRA software (Breitenbach et al., 2012) (Figure S2 in Supporting Information S1). This age model shows that the sample spans continuously a period from ~5,866 to 3,665 yr BP, covering the late part of the mid-Holocene and the early part of the late-Holocene.

3.3. The GZXN Proxy Records

In the GZXND21-1 records, δ^{13}C values range from −10.3 to −12.4‰ and annual lamina thickness varies between 0.02 and 0.7 mm (Table S2 in Supporting Information S1). While the long-term trend of both δ^{13}C and lamina thickness appears stable, a significant periodicity of ~550 yr in both records is outstanding with large amplitudes of ~2‰ and ~0.35 mm, respectively (Figure S4 in Supporting Information S1). There is a significant correlation between GZXND21-1 δ^{13}C and lamina thickness data ($r = -0.15$, $p < 0.001$). Cross-wavelet analysis reveals a prominent anti-phased relationship between the two proxies at the 550-yr period, where more negative δ^{13}C values correspond to thicker laminae (Figure S4 in Supporting Information S1). Considering that band-pass filtering on a specific band can help to eliminate noise and visually compare the phase relationship, a 400–600 FFT band-pass filter ($B.P._{400-600}$) was implemented and the results also show a significant muti-centennial co-variance between δ^{13}C and lamina thickness from ~5,866 to 3,665 yr BP (Figure S6 in Supporting Information S1). A principal component analysis (PCA) was performed on the δ^{13}C and lamina thickness datasets to efficiently discern multi-centennial-scale co-variation patterns (Figure S5 in Supporting Information S1). The first principal component (PC1) clearly shows a ~550-yr periodicity and an in-phase relationship between δ^{13}C and lamina thickness (Figures S6 and S7d in Supporting Information S1). However, the ~550-yr periodicity does not appear significant in the δ^{18}O, Mg/Ca, and Sr/Ca records (Figures S7a–S7c and S8a in Supporting Information S1).

10.1029/2023GL103523

4. Discussion

4.1. Interpretation of Proxies

Carbon isotopes in stalagmites can provide important insights into changes in the local hydroclimate and vegetation (e.g., Fohlmeister et al., 2020; Lechleitner et al., 2021). The carbon in speleothem is derived mainly from three sources: atmospheric CO_2, biogenic soil CO_2, and bedrock. During the growth period of stalagmite GZXND21-1, both the atmospheric pCO_2 (less than 5 ppmv) and isotopic composition of atmospheric CO_2 (a few tenths of a per mil) were virtually constant (Bereiter et al., 2014; Schmitt et al., 2012). Thus, the influence of atmospheric CO_2 on stalagmite $\delta^{13}C$ is negligible. The remaining two carbon sources in the bedrock and biogenic CO_2 are characterized by heavy (usually larger than or close to 0‰) and light $\delta^{13}C$ (usually between −26 and −10 ‰), respectively (e.g., McDermott, 2004). Therefore, variations in stalagmite $\delta^{13}C$ can be influenced in principle by changes in the relative contribution of biogenic soil CO_2 and bedrock, which can be affected subsequently by changes in the local hydroclimate and vegetation conditions.

Similar to most regions in the monsoonal China, our research area is presently covered by C3-type plants, and no evidence has been found that indicates a replacement of C3 plants by C4 plants occurred during the Holocene (e.g., Gong et al., 2019; K. Li et al., 2014). Hence, it is unlikely that the observed $\delta^{13}C$ variations in the speleothem are caused by a shift from C3 (∼−32 to −20‰) to C4 (∼−16 to −9‰) plants due to hydroclimate change in the area. As such, variations in the GZXND21-1 $\delta^{13}C$ record are most likely controlled by the amount of biogenic carbon in the soil. This interpretation is reinforced by the significant negative correlations ($r = -0.15$, $p < 0.001$) and the prominent co-variation on the ∼550-yr periodicity between the $\delta^{13}C$ and lamina thickness records (Figure S4, S6a, and S6c in Supporting Information S1). This is because both $\delta^{13}C$ and speleothem growth rates (lamina thickness) are influenced by the amount of biogenic CO_2 available in the soil. Generally, increased concentration of soil CO_2 due to the high amount of soil biogenic matter can lead to the enhanced dissolution of carbonate bedrock, resulting in higher levels of calcium (Ca^{2+}) in drip water. This, in turn, can cause higher speleothem growth rates and more negative $\delta^{13}C$ (e.g., Fohlmeister et al., 2020; Genty et al., 2001; Kaufmann & Dreybrodt, 2004). The 50–100 cm thick soil layer above GZXN Cave can also increase the residence time of water in the soil and contribute to the equilibrium of carbon isotopes between the dissolved inorganic carbon and soil CO_2, further enhancing the biogenic carbon signal in the dripping water (e.g., Genty et al., 2003, 2006; Jiang et al., 2012). In other words, the various epikarst processes may relatively have minor impacts. This is consistent with the observation that the GZXND21-1 $\delta^{18}O$ (a monsoon intensity proxy, e.g., Cheng et al., 2016, 2022), and trace element ratio (Mg/Ca and Sr/Ca) records exhibit distinct patterns and periodicities different from the $\delta^{13}C$ record (see Section 3.3 for details).

According to modern observations and modelling results, the temperature is the primary driving force behind variations in vegetation and soil microbial activity for a large part of the ASM domain including our research area (e.g., H. Liu et al., 2018, 2020; W. Liu et al., 2020; S. Tao et al., 2022; Z.-Q. Zhang & Zhai, 2022). A record of loss on ignition (a proxy used to calculate variations in organic matter in sediments) from a peat core drilled in the Wumeng Mountain region also suggests that productivity in this area was strongly affected by temperature during the late Holocene (Z.-Q. Zeng et al., 2022). Regarding the dimensionality reduction analysis of local climate, we utilize the PC1 results for our discussion. A strong correlation is also evident between temperature records in central and northern monsoonal China and Greenland ice core $\delta^{18}O$ (a temperature proxy) on a multi-centennial timescale (Figure S4 in Supporting Information S1). Therefore, we propose that the multi-centennial variations in our $\delta^{13}C$ and lamina thickness records are strongly influenced by regional temperature and its impact on soil productivity. Considering the relationship between paleoclimate proxies and the controlling factors of the regional climate model, local rainfall may have merely a weak influence on the multi-centennial variations of $\delta^{13}C$ and lamina thickness (see Text S4 in Supporting Information S1 for details). Nonetheless, it remains an open question to what extent the rainfall has affected the $\delta^{13}C$ and lamina thickness.

4.2. Mechanisms and Teleconnections of the ∼550-Yr Temperature and Vegetation Periodicity

The GZXND21-1 $\delta^{13}C$ and lamina thickness records show significant multi-centennial periodicities between 5,870 and 3,670 yr BP (Figures S4b–S4d in Supporting Information S1), superimposed on their long-term trends. As mentioned above, we suggest that these cyclic changes indicate mainly the temperature and vegetation variations in southwestern China. The $B.P._{400-600}$ filtered PC1 data from $\delta^{13}C$ and lamina thickness show that warm climate "optima" occurred around 5,500, 4,900, 4,350, and 3,800 yr BP, and cold climate at around 5,750, 5,200,

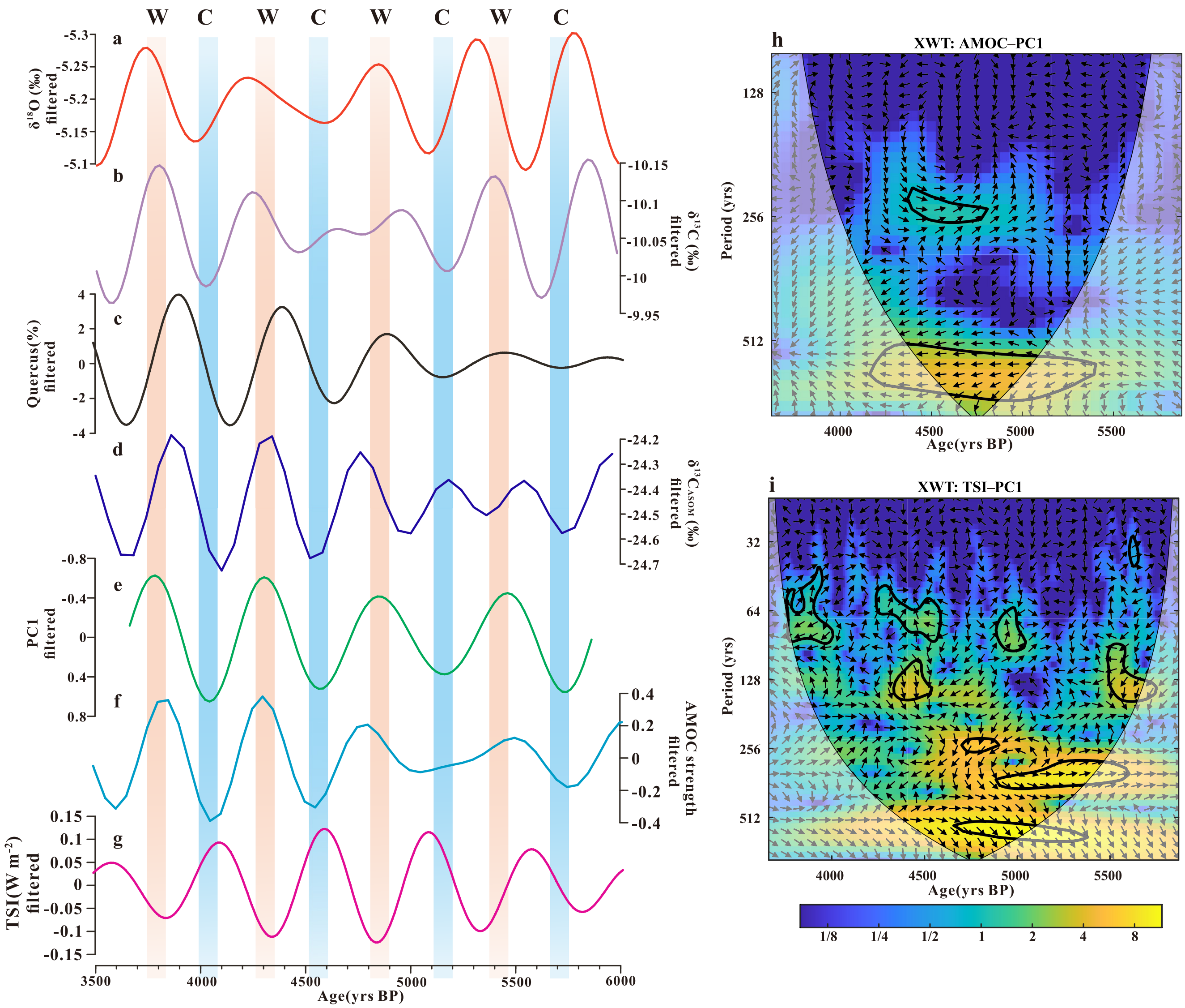

Figure 2. Comparison of multi-centennial variations in different climate records and tree-ring $\Delta^{14}C$ data. (a) and (b) are Jeita Cave $\delta^{18}O$ and $\delta^{13}C$ records (Cheng et al., 2015). (c) The Quercus percentage record from Lake Xiaolongwan (Xu et al., 2019). (d) The $\delta^{13}C_{ASOM}$ record from Heshang Cave (X. Li et al., 2014). (e) The GZXND21-1 PC1 results (this study). (f) North Atlantic Meridional overturning circulation (AMOC) strength data (Ayache et al., 2018; Jomelli et al., 2022). (g) Total solar irradiance (TSI) data (C.-J. Wu et al., 2018). All the records are filtered data ($B.P._{400-600}$). The pink and blue vertical bars represent peak periods of warm (W) and cold (C). (h) and (i) are results of cross-wavelet analysis (calculated using the Acycle package (M. Li et al., 2019)) of the PC1 results with AMOC and TSI records respectively. The black arrows (right/left) indicate the phase relationship of the two records (in/anti-phased). The areas inside the thick line mark the 95% significance level.

4,600, and 4,050 yr BP (Figure 2). Such quasi-periodic ~500–550-yr oscillations of temperature and vegetation are also documented in other well-dated records from northern to central China. For example, in the northwestern margin of the Changbai Mountain in northeastern China, a pollen (Quercus and *Pinus*) record from an annually laminated maar lake shows vegetation zones and temperature fluctuations with a quasi-period of ~500 yr (Xu et al., 2014), which exhibits an in-phase relationship with the filtered ($B.P._{400-600}$) GZXND21-1 PC1 data. In addition, the filtered ($B.P._{400-600}$) $\delta^{13}C$ record of the acid-soluble organic matter ($\delta^{13}C_{ASOM}$) from Heshang Cave, central China (X. Li et al., 2014) also exhibits the ~500–550 yr cyclicity with a nearly in-phase relationship with our PC1 data (Figure 2). Taken together, the ~500–550 yr cyclicity of temperature and vegetation manifests a large spatial scale in monsoonal China around the transition from the mid-to late-Holocene.

The coincidence of the ~550-yr cyclicity in the cosmogenic nuclide record (atmospheric $\Delta^{14}C$), and climate records from northern and central China in the early- and late-Holocene (e.g., Stebich et al., 2015; Y. Wang et al., 2005; Xu et al., 2019, 2020; Zhu et al., 2017) suggests that the presence of the ∼550-yr cycle revealed in the vast ASM domain could be causally linked to solar activity and/or the related atmosphere-ocean processes in the early- and late-Holocene. However, the multi-centennial climate variations from 5,870 to 3,670 yr BP appear complex (Roth & Reijmer, 2005; Zhu et al., 2017). Similar to previous studies (Roth & Reijmer, 2005), the $B.P._{400–600}$ filtered recent data of the total solar irradiance (TSI) (C.-J. Wu et al., 2018) show a nearly anti-phased relation with the proxy data mentioned above (Figures 2e, 2g, and 2i). This observation implies that the ∼550-yr temperature oscillation during the mid-Holocene is caused by internal (but may be not external) climate forcing(s) (e.g., Y. Li & Yang, 2022). A recent study by Jomelli et al. (2022) suggests that changes in the intensity of the Atlantic meridional overturning circulation (AMOC) can have a significant impact on NH temperature during the mid-and late Holocene. In fact, fluctuations in the North Atlantic Deep Water (NADW), which is closely related to the changes in the AMOC, have also shown a periodicity of ∼550 yr during the Holocene (Chapman & Shackleton, 2000). To test this possible teleconnection, we compared our filtered ($B.P._{400–600}$) PC1 results with filtered ($B.P._{400–600}$) AMOC strength reconstructions (Ayache et al., 2018; Jomelli et al., 2022), and found an in-phase relationship between both records (Figures 2e, 2f, and 2h), supporting the idea that the variation of the AMOC may have caused the ∼550-yr oscillation in the YGP during 5,870 to 3,670 yr BP.

Model simulations have shown that the multi-centennial oscillations of the AMOC may be initially stimulated by the solar irradiance (Weber et al., 2014), and in turn instigated by internal mechanism(s), such as the meridional propagation of salinity anomalies in the Atlantic, changes in the Southern Ocean, tropical dynamics, and Arctic sea-ice changes (e.g., Abram et al., 2016; Delworth & Zeng, 2012; Menary et al., 2012). The AMOC oscillations largely affect heat transport to the North Atlantic, and sequentially contribute to the fluctuations in surface air temperatures at different latitudes in NH (Delworth & Zeng, 2012). Moreover, these processes may lead to multi-centennial changes in the North Atlantic Oscillation (e.g., Czaja & Frankignoul, 2002; Rahmstorf et al., 2015; Trouet et al., 2012), which may enlarge the influence of AMOC on China temperature (e.g., Xu et al., 2014). Previous studies also suggest that the AMOC oscillations may be amplified by changes in Antarctic ice sheet discharge, leading to a larger AMOC fluctuation equivalent to ∼1–3 Sv (1 Sv = 10^6 m^3 s^{-1}) freshwater impact or a global temperature fluctuation of ∼0.2–0.6 K (Bakker et al., 2017). Pollen records indicate that the present climate is near the middle phase of a consistent 500–550-yr cycle with a downward trend (Xu et al., 2019). This observation aligns with the recorded weakening of the AMOC by ∼3 ± 1 Sv over the past century (Caesar et al., 2018). Recent modelling results (Jomelli et al., 2022) show this weakening of AMOC may cause a potential cooling of about 0.5°C north of 30°N compared to preindustrial values. If this trend continues, the AMOC weakening may lead to a potential cooling, which in turn would dampen the global warming process to some extent (Jomelli et al., 2022).

The well-dated speleothem $\delta^{13}C$ and $\delta^{18}O$ records from the eastern Mediterranean coastline also show a significant ∼500-yr periodicity (Cheng et al., 2015) in-phased with our YGP records (Figure 2), suggesting that the ∼550-yr cycle may be a large spatial-scale phenomenon. The potential mechanism might be attributed to the AMOC changes. This is because a strengthened (weakened) AMOC will not only result in a temperature increase (decrease) in China, but also lead to a weakened (strengthened) anticyclonic circulation over the Mediterranean via changing the surface temperature, contributing to a long-term increase (decrease) in the wet season Mediterranean precipitation (e.g., Delworth et al., 2022; Stockhecke et al., 2016).

In short, we suggest that the large spatial-scale ∼550-yr climate cycle is likely attributed to the Earth's internal ocean-atmosphere oscillations. However, considering the possible lagged climate responses to external forcings due to the large oceanic memory (e.g., Scaife et al., 2013), we cannot exclude or well assess a potential impact or interplays to internal forcing (e.g., whether the internal forcing overwhelmed the external forcing) of the solar activity, which has a similar cycle of ∼500-yr. As such, more research is still needed to better understand the observed significant ∼500-yr cycles and the underlying internal-external forcings and climate dynamics.

4.3. The Possible Influence of Climate Change on the Neolithic Culture Evolution on the YGP

The unfavourable channel network in the YGP appears to have resulted in the prehistorical civilization in the region being several thousand years behind its neighbors. As a result, the Neolithic culture in the YGP retains many characteristics of the Paleolithic period, namely "Epipaleolithic" (S. Zhang, 2000). The complex topography of the YGP has also led to the Neolithic culture being divided into numerous small cultural and geographic units due to the exchange difficulties among them (W. Wang, 2021). However, a line of evidence from various

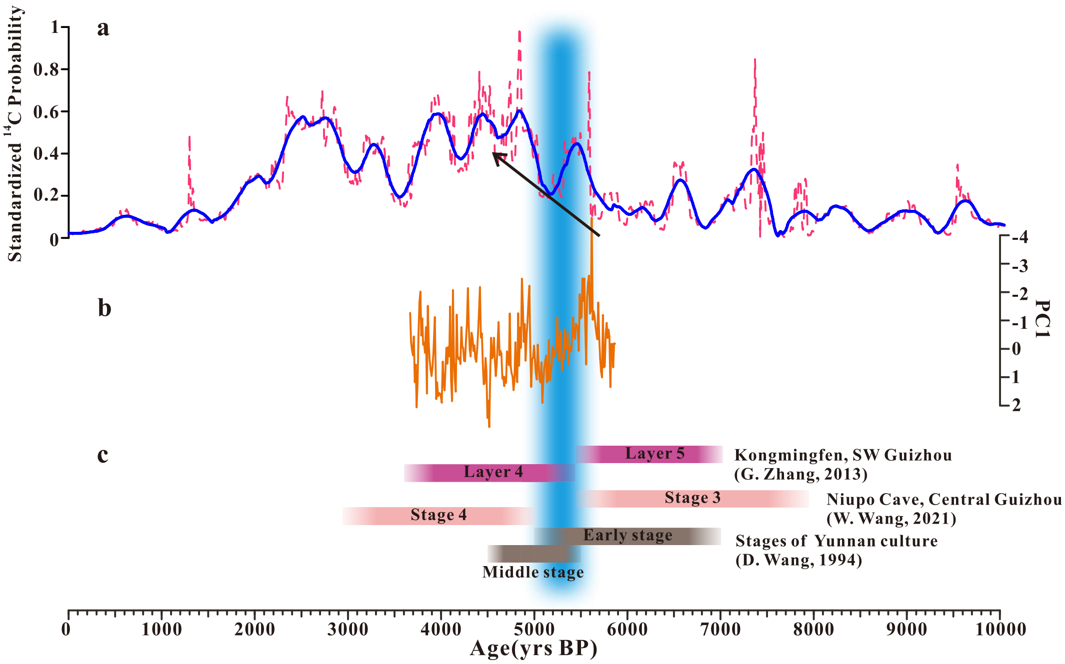

Figure 3. (a) Summed ^{14}C probability (SCP) records in southwestern China over the last 10 kyr (this study). (b) The PC1 results from the GZXN21-1 records. (c) Different stages in the development of the YGP Neolithic culture. The blue bar depicts the first cold event in our records (positive excursion) during ~5,500–5,000 yr BP. The red dotted line and the blue thick line represent the original and Savitzky-Golay 100-point-smoothing SCP records respectively.

archaeological sites in the YGP suggests that the development of instruments of production was widely synchronous around ~5,500–5,000 yr BP (Figure 3). For example, at the Kongmingfen archaeological site in the Beipan River basin (Figure 1), the polished stone tools and potteries are found in the fifth layer dated at ~5,500–5,000 yr BP by ^{14}C age (G. Zhang, 2013). At the Niupo cave site in central Guizhou, the percentage of chipped artifacts dropped significantly and the potteries appeared after 5,500–5,000 yr BP (W. Wang, 2021). Radiocarbon dating shows that the middle stage of the Neolithic culture in Yunnan, which includes the Haimenkou and Yinsuodao sites in the Erhai region and Jianhu basin, respectively, began around 5,500–5,000 yr BP (Wan, 2013; Xue et al., 2022), as evidenced by an increase in the number of polished stone tools and pottery (W. Wang, 2021; Yunnan Institute of Archaeology, 2009). This is consistent with the cultural phases identified by D. Wang (1994). Chen (2020) further suggests that the Neolithic culture in southwestern China commenced at ~5,000 yr BP. In summary, a line of archaeological evidence suggests that 5,500–5,000 yr BP was a critical period in the evolution of prehistorical production implements in the YGP, which occurred in a relatively cold condition with reduced vegetation (Figure 3). This period is also corresponding with the cultural development in eastern China and the emergency of agriculture in both the Sichuan Basin and eastern Qinghai-Tibet Plateau (Jin et al., 2014; W. Wu et al., 2017; Xu et al., 2019).

During 5,700–4,800 yr BP, the population showed an overall growth trend, but experienced a significant decrease between 5,500 and 5,000 yr BP, which is consistent with the "warm-cold-warm" climate states recorded by our PC1 data (Figure 3a and Text S3 in Supporting Information S1). These results suggest that environmental degradation limited the growth of prehistoric populations and may lead to a potential resource scarcity during a colder and vegetation deterioration climate condition. Experimental studies have shown that the use of polishing techniques in manufactures was generally a labor-intensive and time-consuming process in prehistory (e.g., Boydston, 1989). However, this technique had the advantage of producing durable tools and thus significantly improving production efficiency (e.g., Boydston, 1989). We suggest that improvements in technique during ~5,500–5,000 yr BP in YGP may be implying a possible strategy for ancient societies to adapt to the abrupt climate change in the region. While these results suggest a significant role of climate change in the cultural evolution in the YGP, many other factors, such as cultural influences from other regions and agricultural developments, that may have also contributed to this chapter of the prehistorical development in production implements in the region.

5. Conclusions

High-resolution and precisely dated $\delta^{13}C$ and lamina thickness records from the YGP allow us to characterize local vegetation and temperature variations and their pronounced ∼550-yr cycle from 5,870 to 3,670 yr BP. Our analyses reveal that the periodic ∼550-yr temperature and vegetation variations observed in the YGP virtually coincided with the climate changes in northern-central China, the North Atlantic, and the eastern Mediterranean, suggesting that the ∼550-yr climate oscillations may be a large spatial-scale phenomenon. Based on our comparison, the multi-centennial variations in the AMOC, instead of solar activity, may act as an underlying controller for these ∼550-yr climate cycles, possibly through changing the coupled ocean-atmosphere states. In addition, we observed that an evident Neolithic production tools development in the YGP coincides with the first cold event recorded in our record at ∼5,500–5,000 yr BP. This implies that abrupt climate change may play a significant role in the evolution of the prehistorical culture in the region.

Data Availability Statement

The Supporting Information S1 is available through Zenodo (https://doi.org/10.5281/zenodo.7932124) and includes Texts S1–S4, Figures S1–S8 in Supporting Information S1. The speleothem geochemistry and lamina thickness data (Table S2 in Supporting Information S1), the updated ^{14}C database from archaeological sites in southwestern China (Table S3 in Supporting Information S1), the calculated minimal occupation events as the unit of analysis by combining more than one ^{14}C data (Table S4 in Supporting Information S1) and the summed ^{14}C probability (SCP) records (Table S5 in Supporting Information S1) in this publication are available through Dryad (https://doi.org/10.5061/dryad.4tmpg4fg8). The CRU TS v4.05 data (Harris et al., 2020) was obtained from http://climexp.knmi.nl/CRUData/, temperature (1 × 1°) and precipitation (0.5 × 0.5°) data used by our study can be accessed by clicking "cru_ts4.05.1901.2020.tmp.dat_1.nc" and "cru_ts4.05.1901.2020.pre.dat.nc," respectively. Literature data for this research are available in Cheng et al. (2015), Xu et al. (2019), X. Li et al. (2014), Ayache et al. (2018), Jomelli et al. (2022), C.-J. Wu et al. (2018), C. Wang et al. (2014), Zhu et al. (2017). A Matlab-based time-series analysis software, Acycle (M. Li et al., 2019), used for the cross-wavelet analysis, is available through https://acycle.org/downloads/; Past 4.03 software (Hammer et al., 2001), used for the power spectrum analyses, is available through https://www.nhm.uio.no/english/research/resources/past/; OxCal v4.4 software used for calculate the summed ^{14}C probability (SCP), is available through https://c14.arch.ox.ac.uk/oxcal.html; Origin software used for PCA and band-pass filter, is available through https://www.originlab.com/demodownload.aspx.

Acknowledgments

This work is supported by National Nature Science Foundation of China (NSFC) Grants (41888101 and 42150710534) to HC; NSFC Grant (4220021058) and Guizhou Provincial Science and Technology Projects (No. [2020]1Y162) to YL; NSFC Grant (42103005) to LS; NSFC Grant (42050410317) and Postdoctoral Science Foundation of China (2020M683452) to CP.

References

Abram, N. J., McGregor, H. V., Tierney, J. E., Evans, M. N., McKay, N. P., Kaufman, D. S., & Consortium PAGES 2k (2016). Early onset of industrial-era warming across the oceans and continents. *Nature*, *536*(7617), 411–418. https://doi.org/10.1038/nature19082

Ayache, M., Swingedouw, D., Mary, Y., Eynaud, F., & Colin, C. (2018). Multi-centennial variability of the AMOC over the Holocene: A new reconstruction based on multiple proxy-derived SST records. *Global and Planetary Change*, *170*, 172–189. https://doi.org/10.1016/j.gloplacha.2018.08.016

Bakker, P., Clark, P. U., Golledge, N. R., Schmittner, A., & Weber, M. E. (2017). Centennial-scale Holocene climate variations amplified by Antarctic Ice Sheet discharge. *Nature*, *541*(7635), 72–76. https://doi.org/10.1038/nature20582

Bereiter, B., Eggleston, S., Schmitt, J., Nehrbass-Ahles, C., Stocker, T. F., Fischer, H., et al. (2014). Revision of the EPICA Dome C CO_2 record from 800 to 600 kyr before present. *Geophysical Research Letters*, *42*(2), 542–549. https://doi.org/10.1002/2014GL061957

Boydston, R. A. (1989). A cost-benefit study of functionally similar tools. In R. Bradley, T. Earle, I. Hodder, C. Renfrew, J. Sabloff, & A. Sherratt (Eds.), *Time, energy and stone tools* (pp. 67–77). Cambridge University Press.

Breitenbach, S. F. M., Rehfeld, K., Goswami, B., Baldini, J. U. L., Ridley, H. E., Kennett, D. J., et al. (2012). Constructing proxy records from age models (COPRA). *Climate of the Past*, *8*(5), 1765–1779. https://doi.org/10.5194/cp-8-1765-2012

Caesar, L., Rahmstorf, S., Robinson, A., Feulner, G., & Saba, V. (2018). Observed fingerprint of a weakening Atlantic Ocean overturning circulation. *Nature*, *556*(7700), 191–196. https://doi.org/10.1038/s41586-018-0006-5

Cao, L., Zhao, P., Yan, Z., Jones, P., Zhu, Y., Yu, Y., & Tang, G. (2013). Instrumental temperature series in eastern and central China back to the nineteenth century. *Journal of Geophysical Research-Atmospheres*, *118*(15), 8197–8207. https://doi.org/10.1002/jgrd.50615

Chapman, M. R., & Shackleton, N. J. (2000). Evidence of 550-year and 1000-year cyclicities in North Atlantic circulation patterns during the Holocene. *The Holocene*, *10*(3), 287–291. https://doi.org/10.1191/095968300671253196

Chen, S. Q. (2019). *In pursuit of human: Thoughts from prehistoric archaeology*. SDX Joint Publishing Company. (in Chinese).

Chen, S. Q. (2020). *Prehistoric modernization: From hunter-gatherer to the origin of agriculture*. SDX Joint Publishing Company. (in Chinese).

Cheng, H., Edwards, R. L., Shen, C.-C., Polyak, V. J., Asmerom, Y., Woodhead, J., et al. (2013). Improvements in ^{230}Th dating, ^{230}Th and ^{234}U half-life values, and U-Th isotopic measurements by multi-collector inductively coupled plasma mass spectrometry. *Earth and Planetary Science Letters*, *371–372*, 82–91. https://doi.org/10.1016/j.epsl.2013.04.006

Cheng, H., Edwards, R. L., Sinha, A., Spötl, C., Yi, L., Chen, S., et al. (2016). The Asian monsoon over the past 640,000 years and ice age terminations. *Nature*, *534*(7609), 640–646. https://doi.org/10.1038/nature18591

Cheng, H., Li, H., Sha, L., Sinha, A., Shi, Z., Yin, Q., et al. (2022). Milankovitch theory and monsoon. *Innovation*, *3*(6), 100338. https://doi.org/10.1016/j.xinn.2022.100338

Cheng, H., Sinha, A., Verheyden, S., Nader, F. H., Li, X. L., Zhang, P. Z., et al. (2015). The climate variability in northern Levant over the past 20,000 years. *Geophysical Research Letters*, *42*(20), 8641–8650. https://doi.org/10.1002/2015GL065397

Czaja, A., & Frankignoul, C. (2002). Observed impact of Atlantic SST anomalies on the North Atlantic oscillation. *Journal of Climate*, *15*(6), 606–623. https://doi.org/10.1175/1520-0442(2002)015<0606:OIOASA>2.0.CO;2

Dansgaard, W., Johnsen, S. J., Clausen, H. B., Dahl-Jensen, D., Gundestrup, N. S., Hammer, C. U., et al. (1993). Evidence for general instability of past climate from a 250-kyr ice-core record. *Nature*, *364*(6434), 218–220. https://doi.org/10.1038/364218a0

Delworth, T. L., Cooke, W. F., Naik, V., Paynter, D., & Zhang, L. (2022). A weakened AMOC may prolong greenhouse gas–induced Mediterranean drying even with significant and rapid climate change mitigation. *Proceedings of the National Academy of Sciences of the United States of America*, *119*(35), e2116655119. https://doi.org/10.1073/pnas.2116655119

Delworth, T. L., & Zeng, F. (2012). Multicentennial variability of the Atlantic Meridional Overturning Circulation and its climatic influence in a 4000 year simulation of the GFDL CM2.1 climate model. *Geophysical Research Letters*, *39*(13), 1–6. https://doi.org/10.1029/2012GL052107

Ding, Y., & Dai, X. (1994). Temperature variation in China during the last 100 years. *Meteorological Monthly*, *20*, 19–26. (in Chinese).

Domínguez-Villar, D., Baker, A., Fairchild, I. J., & Edwards, R. L. (2012). A method to anchor floating chronologies in annually laminated speleothems with U-Th dates. *Quaternary Geochronology*, *14*, 57–66. https://doi.org/10.1016/j.quageo.2012.04.019

Dong, X., Kathayat, G., Rasmussen, S. O., Svensson, A., Severinghaus, J. P., Li, H., et al. (2022). Coupled atmosphere-ice-ocean dynamics during Heinrich Stadial 2. *Nature Communications*, *13*(1), 5867. https://doi.org/10.1038/s41467-022-33583-4

Fleitmann, D., Burns, S. J., Mudelsee, M., Neff, U., Kramers, J., Mangini, A., & Matter, A. (2003). Holocene forcing of the Indian monsoon recorded in a stalagmite from Southern Oman. *Science*, *300*(5626), 1737–1739. https://doi.org/10.1126/science.1083130

Fohlmeister, J., Voarintsoa, N. R. G., Lechleitner, F. A., Boyd, M., Brandtstätter, S., Jacobson, M. J., & Oster, J. L. (2020). Main controls on the stable carbon isotope composition of speleothems. *Geochimica et Cosmochimica Acta*, *279*, 67–87. https://doi.org/10.1016/j.gca.2020.03.042

Genty, D., Baker, A., & Vokal, B. (2001). Intra- and inter-annual growth rate of modern stalagmites. *Chemical Geology*, *176*(1–4), 191–212. https://doi.org/10.1016/S0009-2541(00)00399-5

Genty, D., Blamart, D., Ghaleb, B., Plagnes, V., Causse, C., Bakalowicz, M., et al. (2006). Timing and dynamics of the last deglaciation from European and North African $\delta^{13}C$ stalagmite profiles—Comparison with Chinese and South Hemisphere stalagmites. *Quaternary Science Reviews*, *25*(17–18), 2118–2142. https://doi.org/10.1016/j.quascirev.2006.01.030

Genty, D., Blamart, D., Ouahdi, R., Gilmour, M., Baker, A., Jouzel, J., & Van-Exter, S. (2003). Precise dating of Dansgaard-Oeschger climate oscillations in western Europe from stalagmite data. *Nature*, *421*(6925), 833–837. https://doi.org/10.1038/nature01391

Gong, X., Chen, C., Tang, Y., Huang, K., Yue, Y., Liang, K., & Zheng, Z. (2019). Palaeoenvironment changes during the past 21 ka inferred from organic geochemical records of Caohai Lake, Guizhou Province. *Journal of Palaeogeography*, *21*(6), 1025–1034. (Chinese edition with English abstract). https://doi.org/10.7605/gdlxb.2019.06.070

Hammer, Ø., Harper, D. A. T., & Ryan, P. D. (2001). PAST: Paleontological statistics software package for education and data analysis. *Palaeontologia Electronica*, *4*(1), 9. http://palaeo-electronica.org/2001_1/past/issue1_01.htm

Harris, I., Osborn, T. J., Jones, P., & Lister, D. (2020). Version 4 of the CRU TS monthly high-resolution gridded multivariate climate dataset. *Scientific Data*, *7*(1), 109. https://doi.org/10.1038/s41597-020-0453-3

Hoelzmann, P., Keding, B., Berke, H., Kröpelin, S., & Kruse, H.-J. (2001). Environmental change and archaeology: Lake evolution and human occupation in the Eastern Sahara during the Holocene. *Palaeogeography, Palaeoclimatology, Palaeoecology*, *169*(3–4), 193–217. https://doi.org/10.1016/S0031-0182(01)00211-5

Jiang, X.-Y., Li, Z.-Z., Li, J.-Q., Kong, X.-G., & Guo, Y. (2012). Stalagmite $\delta^{18}O$ record from Yuhua cave over the past 500 Years and its regional climate significance. *Scientia Geographica Sinica*, *32*(2), 207–212. (Chinese edition with English abstract). https://doi.org/10.13249/j.cnki.sgs.2012.02.018

Jin, T., Liu, X., Min, R., & Wu, X. (2014). A Study on flotation result of plant remains in the Dadunzi site of Yuanmou, Yunan. *Jianghan Archaeology*, *132*, 109–113. (Chinese edition with English abstract).

Jomelli, V., Swingedouw, D., Vuille, M., Favier, V., Goehring, B., Shakun, J., et al. (2022). In-phase millennial-scale glacier changes in the tropics and North Atlantic regions during the Holocene. *Nature Communications*, *13*(1), 1419. https://doi.org/10.1038/s41467-022-28939-9

Kathayat, G., Cheng, H., Sinha, A., Yi, L., Li, X., Zhang, H., et al. (2017). The Indian monsoon variability and civilization changes in the Indian subcontinent. *Science Advances*, *3*(12), e1701296. https://doi.org/10.1126/sciadv.1701296

Kaufmann, G., & Dreybrodt, W. (2004). Stalagmite growth and palaeo-climate: An inverse approach. *Earth and Planetary Science Letters*, *224*(3–4), 529–545. https://doi.org/10.1016/j.epsl.2004.05.020

Lechleitner, F. A., Day, C. C., Kost, O., Wilhelm, M., Haghipour, N., Henderson, G. M., & Stoll, H. M. (2021). Stalagmite carbon isotopes suggest deglacial increase in soil respiration in western Europe driven by temperature change. *Climate of the Past*, *17*(5), 1903–1918. https://doi.org/10.5194/cp-17-1903-2021

Li, H., Xu, D., Shen, C., Cui, A., Zuo, X., Dong, Y., et al. (2021). Multi-centennial climate cycles and their impact on the Tubo dynasty in the southern Tibetan Plateau. *Palaeogeography, Palaeoclimatology, Palaeoecology*, *578*(7), 110584. https://doi.org/10.1016/j.palaeo.2021.110584

Li, K., Zhu, C., Jiang, F., Li, B., Wang, X., Cao, B., & Zhao, X. (2014). Archaeological sites distribution and its physical environmental settings between ca 260−2.2 ka BP in Guizhou, Southwest China. *Journal of Geographical Sciences*, *24*(3), 526–538. https://doi.org/10.1007/s11442-014-1104-4

Li, M., Hinnov, L., & Kump, L. (2019). Acycle: Time-series analysis software for paleoclimate research and education. *Computers & Geosciences*, *127*, 12–22. https://doi.org/10.1016/j.cageo.2019.02.011

Li, N., Li, M., Sack, D., Kang, W., Song, L., Yang, Y., et al. (2020). Diatom evidence for mid-Holocene peatland water-table variations and their possible link to solar forcing. *Science of the Total Environment*, *725*, 138272. https://doi.org/10.1016/j.scitotenv.2020.138272

Li, X., Hu, C., Huang, J., Xie, S., & Baker, A. (2014). A 9000-year carbon isotopic record of acid-soluble organic matter in a stalagmite from Heshang Cave, central China: Paleoclimate implications. *Chemical Geology*, *388*, 71–77. https://doi.org/10.1016/j.chemgeo.2014.08.029

Li, Y., & Yang, H. (2022). A theory for self-sustained multicentennial oscillation of the Atlantic meridional overturning circulation. *Journal of Climate*, *35*(18), 5883–5896. https://doi.org/10.1175/JCLI-D-21-0685.1

Li, Y. W., Pérez-Mejías, C., Zhao, J., Li, H., Zhang, H., Lu, J., et al. (2022). Indian summer monsoon variations during the Younger Dryas as revealed by a laminated stalagmite record from the Tibetan Plateau. *Quaternary Science Reviews*, *278*, 107375. https://doi.org/10.1016/j.quascirev.2022.107375

Liu, H., Jiao, F., Yin, J., Li, T., Gong, H., Wang, Z., & Lin, Z. (2020). Nonlinear relationship of vegetation greening with nature and human factors and its forecast—A case study of southwest China. *Ecological Indicators*, *111*, 106009. https://doi.org/10.1016/j.ecolind.2019.106009

Liu, H., Zhang, M., Lin, Z., & Xu, X. (2018). Spatial heterogeneity of the relationship between vegetation dynamics and climate change and their driving forces at multiple time scales in Southwest China. *Agricultural and Forest Meteorology*, *256*(257), 10–21. https://doi.org/10.1016/j.agrformet.2018.02.015

Liu, W., Wang, G., Yu, M., Chen, H., Jiang, Y., Yang, M., & Shi, Y. (2020). Projecting the future vegetation–climate system over East Asia and its RCP-dependence. *Climate Dynamics*, *55*(9–10), 2725–2742. https://doi.org/10.1007/s00382-020-05411-2

McDermott, F. (2004). Palaeo-climate reconstruction from stable isotope variations in speleothems: A review. *Quaternary Science Reviews*, *23*(7–8), 901–918. https://doi.org/10.1016/j.quascirev.2003.06.021

McDermott, F., Mattey, D. P., & Hawkesworth, C. (2001). Centennial-scale Holocene climate variability revealed by a high-resolution speleothem $\delta^{18}O$ record from SW Ireland. *Science*, *294*(5545), 1328–1331. https://doi.org/10.1126/science.1063678

Menary, M. B., Park, W., Lohmann, K., Vellinga, M., Palmer, M. D., Latif, M., & Jungclaus, J. H. (2012). A multimodel comparison of centennial Atlantic meridional overturning circulation variability. *Climate Dynamics*, *38*(11–12), 2377–2388. https://doi.org/10.1007/s00382-011-1172-4

Rahmstorf, S., Box, J. E., Feulner, G., Mann, M. E., Alexander, R., Rutherford, S., & Schaffernicht, E. J. (2015). Exceptional twentieth-century slowdown in Atlantic Ocean overturning circulation. *Nature Climate Change*, *5*, 475–480. https://doi.org/10.1038/nclimate2554

Ren, G., Ding, Y., & Tang, G. (2017). An overview of mainland China temperature change research. *Journal of Meteorological Research*, *31*(1), 3–16. https://doi.org/10.1007/s13351-017-6195-2

Roth, S., & Reijmer, J. J. G. (2005). Holocene millennial to centennial carbonate cyclicity recorded in slope sediments of the Great Bahama Bank and its climatic implications. *Sedimentology*, *52*(1), 161–181. https://doi.org/10.1111/j.1365-3091.2004.00684.x

Scaife, A. A., Ineson, S., Knight, J. R., Gray, L., Kodera, K., & Smith, D. M. (2013). A mechanism for lagged North Atlantic climate response to solar variability. *Geophysical Research Letters*, *40*(2), 434–439. https://doi.org/10.1002/grl.50099

Schmitt, J., Schneider, R., Elsig, J., Leuenberger, D., Lourantou, A., Chappellaz, J., et al. (2012). Carbon isotope constraints on the deglacial CO_2 rise from ice cores. *Science*, *336*(6082), 711–714. https://doi.org/10.1126/science.1217161

Stebich, M., Rehfeld, K., Schlütz, F., Tarasov, P. E., Liu, J., & Mingram, J. (2015). Holocene vegetation and climate dynamics of NE China based on the pollen record from Sihailongwan Maar Lake. *Quaternary Science Reviews*, *124*, 275–289. https://doi.org/10.1016/j.quascirev.2015.07.021

Stockhecke, M., Timmermann, A., Kipfer, R., Haug, G. H., Kwiecien, O., Friedrich, T., et al. (2016). Millennial to orbital-scale variations of drought intensity in the Eastern Mediterranean. *Quaternary Science Reviews*, *133*, 77–95. https://doi.org/10.1016/j.quascirev.2015.12.016

Stuiver, M., Grootes, P. M., & Braziunas, T. F. (1995). The GISP2 $\delta^{18}O$ climate record of the past 16,500 years and the role of the sun, ocean and volcanoes. *Quaternary Research*, *44*(3), 341–354. https://doi.org/10.1006/qres.1995.1079

Sun, Y., Zhang, X., Ren, G., Zwiers, F. W., & Hu, T. (2016). Contribution of urbanization to warming in China. *Nature Climate Change*, *6*(7), 706–709. https://doi.org/10.1038/nclimate2956

Tao, S., Peng, W., & Xiang, J. (2022). Spatiotemporal variations and driving mechanisms of vegetation coverage in the Wumeng Mountainous Area, China. *Ecological Informatics*, *70*, 101737. https://doi.org/10.1016/j.ecoinf.2022.101737

Tao, S. Y., & Chen, L. (1987). A review of recent research on the East Asia summer monsoon in China. In C.-P. Chang & T.-N. Krishnamurti (Eds.), *Monsoon meteorology* (pp. 60–92). Oxford University Press.

Trouet, V., Scourse, J. D., & Raible, C. C. (2012). North Atlantic storminess and Atlantic meridional overturning circulation during the last millennium: Reconciling contradictory proxy records of NAO variability. *Global and Planetary Change*, *84*(85), 48–55. https://doi.org/10.1016/j.gloplacha.2011.10.003

Wan, J. (2013). *Prehistoric culture of Cang'er area*. Cultural Relics Press. (in Chinese).

Wang, C., Lu, H., Zhang, J., Gu, Z., & He, K. (2014). Prehistoric demographic fluctuations in China inferred from radiocarbon data and their linkage with climate change over the past 50,000 years. *Quaternary Science Reviews*, *98*, 45–59. https://doi.org/10.1016/j.quascirev.2014.05.015

Wang, D. (1994). A further typological study on the Neolith culture in Yunnan Province. In W. Huo, Y. Li, & Y. Shi (Eds.), *Tibetan archaeology, Series 1* (pp. 91–108). Sichuan University Press. (Chinese edition with English abstract).

Wang, W. (2021). *One hundred years' history of Chinese archaeology (1921–2021)* (Vol. 1(3), pp. 1050–1300). China Social Sciences Press. (in Chinese).

Wang, Y., Cheng, H., Edwards, R. L., He, Y., Kong, X., An, Z., et al. (2005). The Holocene Asian monsoon: Links to solar changes and North Atlantic climate. *Science*, *308*(5723), 854–857. https://doi.org/10.1126/science.1106296

Weber, M. E., Clark, P. U., Kuhn, G., Timmermann, A., Sprenk, D., Gladstone, R., et al. (2014). Millennial-scale variability in Antarctic ice-sheet discharge during the last deglaciation. *Nature*, *510*(7503), 134–138. https://doi.org/10.1038/nature13397

Wu, C.-J., Krivova, N. A., Solanki, S. K., & Usoskin, I. G. (2018). Solar total and spectral irradiance reconstruction over the last 9000 years. *Astronomy & Astrophysics*, *620*, A120. https://doi.org/10.1051/0004-6361/201832956

Wu, W., Zheng, H., Hou, M., & Ge, Q. (2017). The 5.5 cal ka BP climate event, population growth, circumscription and the emergence of the earliest complex societies in China. *Science China Earth Sciences*, *61*(2), 134–148. https://doi.org/10.1007/s11430-017-9157-1

Xu, D., Lu, H., Chu, G., Liu, L., Shen, C., Li, F., et al. (2019). Synchronous 500-year oscillations of monsoon climate and human activity in Northeast Asia. *Nature Communications*, *10*(1), 4105. https://doi.org/10.1038/s41467-019-12138-0

Xu, D., Lu, H., Chu, G., Shen, C., Li, F., Wu, J., et al. (2020). Asynchronous 500-year summer monsoon rainfall cycles between Northeast and Central China during the Holocene. *Global and Planetary Change*, *195*, 103324. https://doi.org/10.1016/j.gloplacha.2020.103324

Xu, D., Lu, H., Chu, G., Wu, N., Shen, C., Wang, C., & Mao, L. (2014). 500-year climate cycles stacking of recent centennial warming documented in an East Asian pollen record. *Scientific Reports*, *4*(1), 3611. https://doi.org/10.1038/srep03611

Xue, Y., Martello, R. D., Qin, L., Stevens, C. J., Min, R., & Fuller, D. Q. (2022). Post-Neolithic broadening of agriculture in Yunnan, China: Archaeobotanical evidence from Haimenkou. *Archaeological Research in Asia*, *30*, 100364. https://doi.org/10.1016/j.ara.2022.100364

Yunnan Institute of Archaeology. (2009). *Explore historical footprints to protect cultural heritage — commemorating the 50th anniversary of the Yunnan Provincial Institute of Cultural Relics and Archaeology* (pp. 41–47). Yunnan Education Press.

Zeng, M., Zeng, Q., Peng, H., Wu, Y., Li, Y., Song, Y., et al. (2022). Late Holocene hydroclimatic changes inferred from a karst peat archive in the western Guizhou Plateau, SW China. *Journal of Asian Earth Sciences*, *229*, 105179. https://doi.org/10.1016/j.jseaes.2022.105179

Zhang, G. (2013). *The preliminary study of Neolithic remains form Beipan River basin, Guizhou* (Master's thesis). CNKI, Northwest University. Retrieved from (https://kns.cnki.net/kcms2/article/abstract?v=3uoqIhG8C475KOm_zrgu4lQARvep2SAk9z9MrcM-rOU4mSkGl_LWf4Nn-1WUE2dl4aR1mEddxb_ccq-P9xXSMGehT9F619iKi&uniplatform=NZKPT). (Chinese edition with English abstract)

Zhang, S. (2000). The Epipaleolithic in China. *Journal of East Asian Archaeology*, *1*, 51–66. https://doi.org/10.1163/156852300509790

Zhang, Z.-Q., & Zhai, P.-M. (2022). Numerical simulation of the effects of global warming on vegetation in Asia. *Advances in Climate Change Research*, *13*(5), 688–699. https://doi.org/10.1016/j.accre.2022.08.005

Zhu, Z., Feinberg, J. M., Xie, S., Bourne, M. D., Huang, C., Hu, C., & Cheng, H. (2017). Holocene ENSO-related cyclic storms recorded by magnetic minerals in speleothems of central China. *Proceedings of the National Academy of Sciences of the United States of America*, *114*(5), 852–857. https://doi.org/10.1073/pnas.1610930114

References From the Supporting Information

Brown, W. A. (2015). Through a filter, darkly: Population size estimation, systematic error, and random error in radiocarbon-supported demographic temporal frequency analysis. *Journal of Archaeologial Science*, *53*, 133–147. https://doi.org/10.1016/j.jas.2014.10.013

Chaput, M. A., & Gajewski, K. (2016). Radiocarbon dates as estimates of ancient human population size. *Anthropocene*, *15*, 3–12. https://doi.org/10.1016/j.ancene.2015.10.002

Cheng, H., Edwards, R. L., Hoff, J., Gallup, C. D., Richards, D. A., & Asmerom, Y. (2000). The half-lives of uranium-234 and thorium-230. *Chemical Geology*, *169*(1–2), 17–33. https://doi.org/10.1016/S0009-2541(99)00157-6

Edwards, R. L., Chen, J., & Wasserburg, G. J. (1987). ^{238}U–^{234}U–^{230}Th–^{232}Th systematics and the precise measurement of time over the past 500,000 years. *Earth and Planetary Science Letters*, *81*(2–3), 175–192. https://doi.org/10.1016/0012-821X(87)90154-3

Fairchild, I. J., & Treble, P. C. (2009). Trace elements in speleothems as recorders of environmental change. *Quaternary Science Reviews*, *28*(5–6), 449–468. https://doi.org/10.1016/j.quascirev.2008.11.007

Gamble, C., Davies, W., Pettitt, P., Hazelwood, L., & Richards, M. (2005). The archaeological and genetic foundations of the European population during the late glacial: Implications for "agricultural thinking". *Cambridge Archaeological Journal*, *15*(2), 193–223. https://doi.org/10.1017/S0959774305000107

Huo, H., & Sun, C. (2021). Spatiotemporal variation and influencing factors of vegetation dynamics based on geodetector: A case study of the northwestern Yunnan plateau, China. *Ecological Indicators*, *130*, 108005. https://doi.org/10.1016/j.ecolind.2021.108005

Johnson, K. R., Hu, C., Belshaw, N. S., & Henderson, G. M. (2006). Seasonal trace-element and stable-isotope variations in a Chinese speleothem: The potential for high-resolution paleomonsoon reconstruction. *Earth and Planetary Science Letters*, *244*(1–2), 394–407. https://doi.org/10.1016/j.epsl.2006.01.064

Kosaka, Y., Chowdary, J. S., Xie, S.-P., Min, Y.-M., & Lee, J.-Y. (2012). Limitations of seasonal predictability for summer climate over East Asia and the Northwestern Pacific. *Journal of Climate*, *25*(21), 7574–7589. https://doi.org/10.1175/JCLI-D-12-00009.1

Li, H., Cheng, H., Wang, J., Tian, Y., & Ning, Y. (2018). Applications of laser induced breakdown spectroscopy to paleoclimate research: Reconstructing speleothem trace element records. *Quaternary Sciences*, *38*, 1549–1551. (Chinese edition with English abstract). https://doi.org/10.11928/j.issn.1001-7410.2018.06.21

Li, H., Sinha, A., André, A. A., Spötl, C., Vonhof, H. B., Meunier, A., et al. (2020). A multimillennial climatic context for the megafaunal extinctions in Madagascar and Mascarene Islands. *Science Advances*, *6*(42), eabb2459. https://doi.org/10.1126/sciadv.abb2459

McMillan, E. A., Fairchild, I. J., Frisia, S., Borsato, A., & McDermott, F. (2005). Annual trace element cycles in calcite–aragonite speleothems: Evidence of drought in the western Mediterranean 1200–1100 yr BP. *Journal of Quaternary Science*, *20*(5), 423–433. https://doi.org/10.1002/jqs.943

Michczyńska, D. J., & Pazdur, A. (2004). Shape analysis of cumulative probability density function of radiocarbon dates set in the study of climate change in late glacial and holocene. *Radiocarbon*, *46*(2), 733–744. https://doi.org/10.1017/S0033822200035773

Nitta, T. (1987). Convective activities in the tropical western Pacific and their impact on the Northern Hemisphere summer circulation. *Journal of the Meteorological Society of Japan*, *65*(3), 373–390. https://doi.org/10.2151/jmsj1965.65.3_373

Qi, X., Cui, C., Peng, Y., Zhang, X., Yang, Z., Zhong, H., et al. (2013). Genetic evidence of Paleolithic colonization and Neolithic expansion of modern humans on the Tibetan Plateau. *Molecular Biology and Evolution*, *30*(8), 1761–1778. https://doi.org/10.1093/molbev/mst093

Rasmussen, S. O., Bigler, M., Blockley, S. P., Blunier, T., Buchardt, S. L., Clausen, H. B., et al. (2014). A stratigraphic framework for abrupt climatic changes during the last glacial period based on three synchronized Greenland ice-core records: Refining and extending the INTIMATE event stratigraphy. *Quaternary Science Reviews*, *106*, 14–28. https://doi.org/10.1016/j.quascirev.2014.09.007

Shennan, S., & Edinborough, K. (2007). Prehistoric population history: From the late glacial to the late Neolithic in central and northern Europe. *Journal of Archaeological Science*, *34*(8), 1339–1345. https://doi.org/10.1016/j.jas.2006.10.031

Surovell, T. A., & Brantingham, P. J. (2007). A note on the use of temporal frequency distributions in studies of prehistoric demography. *Journal of Archaeological Science*, *34*(11), 1868–1877. https://doi.org/10.1016/j.jas.2007.01.003

Surovell, T. A., Finley, B. J., Smith, G. M., Brantingham, P. J., & Kelly, R. (2009). Correcting temporal frequency distributions for taphonomic bias. *Journal of Archaeological Science*, *36*(8), 1715–1724. https://doi.org/10.1016/j.jas.2009.03.029

Tan, M., Baker, A., Genty, D., Smith, C., Esper, J., & Cai, B. (2006). Applications of stalagmite laminae to paleoclimate reconstructions: Comparison with dendrochronology/climatology. *Quaternary Science Reviews*, *25*(17–18), 2103–2117. https://doi.org/10.1016/j.quascirev.2006.01.034

Wang, J., Wang, K., Zhang, M., & Zhang, C. (2015). Impacts of climate change and human activities on vegetation cover in hilly southern China. *Ecological Engineering*, *81*, 451–461. https://doi.org/10.1016/j.ecoleng.2015.04.022

Williams, A. N. (2012). The use of summed radiocarbon probability distributions in archaeology: A review of methods. *Journal of Archaeological Science*, *39*(3), 578–589. https://doi.org/10.1016/j.jas.2011.07.014

Zhang, H., Zhang, J., Cheng, H., Edwards, R. L., Cai, Y., Liu, B., et al. (2021). Collapse of the Liangzhu and other Neolithic cultures in the lower Yangtze region in response to climate change. *Science Advances*, *7*(48), eabj9275. https://doi.org/10.1126/sciadv.abj9275

Zhang, J., Zhao, K., Wang, Y., Kong, X., Shao, X., Liang, Y., et al. (2021). Modulation of centennial-scale hydroclimate variations in the middle Yangtze River Valley by the East Asian-Pacific pattern and ENSO over the past two millennia. *Earth and Planetary Science Letters*, *576*, 117220. https://doi.org/10.1016/j.epsl.2021.117220

Zhao, J., & Cheng, H. (2017). Applications of laser scanning confocal microscope to paleoclimate research: Characterizing and counting laminae. *Quaternary Sciences*, *37*(6), 1472–1474. (Chinese edition with English abstract). https://doi.org/10.11928/j.issn.1001-7410.2017.06.28